Inverse scattering method for transfer reactions

M. Eberspächer,[1] K. Amos,[1] and B. Apagyi[2]
[1]*School of Physics, The University of Melbourne, Victoria 3010, Australia*
[2]*Institute of Physics, Technical University, Budapest, Hungary*
(Received 16 August 2000; published 13 November 2000)

We extend a modified Newton-Sabatier method for the solution of the fixed energy, coupled channels, inverse scattering problem to deal with a set of cluster transfer reactions. The method is tested by using analytic model potentials for the transfer reaction $^{16}O(\alpha,^{8}Be)^{12}C$. For low energy scattering we show that inclusion of *S* matrices for nonphysical, noninteger angular momenta are required to find stable solutions. The possibility of application to actual experimental data is discussed.

PACS number(s): 24.10.Eq, 24.10.Ht, 25.70.Hi, 03.65.Nk

I. INTRODUCTION

In an earlier work [1], the modified Newton-Sabatier (NS) method [2] for the solution of the inverse scattering problem (ISP) [3,4] at fixed energy [5] was extended from the single channel (elastic scattering) theory to the case of coupled channels. But this extended method, as it was developed, has two handicaps. First, the coupling potentials must not depend on the angular momentum, i.e., the channel coupling interaction must not couple the intrinsic angular momenta to the orbital angular momentum. Only monopole transitions then may be described exactly with this method. However, an approximation scheme has been proposed recently to treat dipole and quadrupole interactions [6]. Second, the method requires a complete *S* matrix as input data. In general that is not obtainable from experiments as the projectile and target in the incoming channel always are in their respective ground states. Consequently only one row of the *S* matrix can be obtained from experimental angular differential cross sections; namely that describing excitation from the elastic channel. The missing information, usually the larger part of the *S* matrix, would need to be added by using known symmetries, physical reasoning, or outright bias. Nevertheless, test case analyses using specific model forms of coupling potentials showed that the upgraded (approximate) method of coupled channels inversion could reproduce the known input with high accuracy. The problem of defining the complete *S* matrix solely from data and *a priori* knowledge remains for future study.

Herein we show that the coupled channel inversion method [1] can be extended also to deal with transfer reactions. Under certain circumstances the complete *S* matrix for that may be given by experiment. Transfer reactions, in which one or more nucleons are transferred between the scattering partners, can be described in terms of the coupled channel formalism as two elastic channels coupled by two transfer reactions. In direct transfer reactions only a small part of the kinetic energy from the incoming channel is transferred to the internal degrees of freedom of the fragments. If all fragments of that coupled system are in the ground state the complete *S* matrix may be measured in the experiment. Also, if one considers the transfer of a spinless fragment, for example, the transfer of an α particle from an even mass nucleus, the interaction potential will be independent of the angular momentum and the basic (monopole) inversion theory need not be approximated.

In this paper, we develop and use the modified NS method for the solution of the ISP at fixed energy with coupled channels for the case of transfer reactions. Not all such scattering can be so treated, however. For example, deep inelastic transfer reactions usually need to be described by nonlocal interactions, whereas the modified NS method yields local potentials only. Even so, the method proposed in this paper can be viewed as a localization procedure for such transfer potentials.

In Sec. II the coupled Schrödinger equations for the transfer reactions are specified and the two coupled channels are defined. In Sec. III the modified NS method is extended to the case of transfer reactions. The well known transformation of the *S* matrix to reduce the ISP problem of charged particle scattering to one of neutral particle scattering [7,8] is applied for the case of transfer reactions in Sec. IV. The equations needed for the solution of the ISP for transfer reactions with neutral particles are given in Sec. V. A first application of the method to the $^{16}O(\alpha,^{8}Be)^{12}C$ reaction is shown in Sec. VI, while in Sec. VII the possibility of improving the inversion process by using nonphysical *S* matrix elements is discussed. This discussion follows the findings of a recent study [9] with the modified NS method for the solution of the single channel elastic ISP at fixed energy. It was shown therein that, for low energy scattering when very few partial waves contribute significantly to the scattering, additional and nonphysical *S* matrix elements are essential to get sensible results. A summary of these studies and conclusions we may draw from this new work follow in Sec. VIII.

II. THE SCHRÖDINGER EQUATION AND THE DEFINITION OF THE CHANNELS

We consider two elastic scattering processes, $A(a,a)A$ and $B(b,b)B$, coupled by the two transfer reactions, $A(a,b)B$ and $B(b,a)A$, so that the complete coupled scattering system and its scattering matrices can be represented in a 2×2 form of

$$\begin{pmatrix} A(a,a)A & A(a,b)B \\ B(b,a)A & B(b,b)B \end{pmatrix}. \tag{1}$$

The mass and charge numbers of projectile and target in channel α we denote by A_p^α, A_t^α, Z_p^α, and Z_t^α, respectively. We limit consideration to the case of transfer reactions in which all fragments are in their ground states which all have zero intrinsic spin ($J_\alpha=0$). Then the orbital angular momenta of relative motion l_α is equal to the total angular momentum, $I(=l_\alpha\otimes J_\alpha)$. In some applications we include nonphysical (noninteger) angular momentum partial waves.

With the supposition that the potential matrix is of local form, the Schrödinger equations for the coupled channels problem are

$$\sum_{\beta=1}^{2} D^V_{\alpha\beta}(r)R^I_{\beta n}(r)=I(I+1)R^I_{\alpha n}(r), \tag{2}$$

where the differential operators are

$$D^V_{\alpha\beta}(r)=r^2\frac{\hbar^2}{2\mu_\alpha}\left\{\left[\frac{\hbar^2}{2\mu_\alpha}\frac{d^2}{dr^2}+E-\varepsilon_\alpha\right]\delta_{\alpha\beta}-V_{\alpha\beta}(r)\right\}, \tag{3}$$

in which μ_α is the channel dependent reduced mass,

$$\mu_\alpha=\frac{A_p^\alpha A_t^\alpha}{A_p^\alpha+A_t^\alpha}m_u\,.$$

m_u is the atomic mass unit. As we do not allow angular momentum coupling, the potential matrix $V_{\alpha\beta}(r)$ does not depend on I. Also we suppose that the excitation energy ε_α is 0 MeV in the first (incident ground state) channel ($\alpha=1$), and equal to the Q-value of the transfer reaction in the second channel ($\alpha=2$). The radial wave functions of relative motion are $R^I_{\alpha n}(r)$ where the index $n(=1,2)$ identifies the two degenerate but linearly independent solutions in each channel. The presumption is that, beyond R_{int}, the forms of the scattering wave functions are known from measurement. The ISP then can be stated thus: *Given the asymptotic wave functions, $R^I_{\alpha n}(r>R_{int})$, find the potential matrix, $V_{\alpha\beta}(r)$ for $r<R_{int}$.*

III. THE MODIFIED NEWTON-SABATIER METHOD

To solve this ISP problem, it is useful to introduce a symmetric reference potential matrix, $V^0_{\alpha\beta}(r)=V^0_{\beta\alpha}(r)$, for which $R^{0I}_{\alpha n}(r)$ are the reference solutions of the reference Schrödinger equation

$$\sum_{\beta=1}^{2} D^{V_0}_{\alpha\beta}(r)R^{0I}_{\beta n}(r)=I(I+1)R^{0I}_{\alpha n}(r), \tag{4}$$

with the reference differential operator

$$D^{V_0}_{\alpha\beta}(r)=r^2\frac{2\mu_\alpha}{\hbar^2}\left\{\left[\frac{\hbar^2}{2\mu_\alpha}\frac{d^2}{dr^2}+E-\varepsilon_\alpha\right]\delta_{\alpha\beta}-V^0_{\alpha\beta}(r)\right\}. \tag{5}$$

In terms of these solutions, which are assumed known on the whole real axis, $0\leqslant r\leqslant\infty$, the wave functions of the sought potential matrix can be written

$$R^I_{\alpha n}(r)=R^{0I}_{\alpha n}(r)-\sum_{\beta=1}^{2}\int_0^r K^{VV_0}_{\alpha\beta}(r,r')R^{0I}_{\beta n}(r')\frac{1}{r'^2}dr'. \tag{6}$$

This ansatz is an extension of the Povzner-Levitan representation [5] for the description of wave functions for coupled channels [1]. It has been shown [10] that functions defined by Eq. (6) fulfill the Schrödinger equations, Eq. (2), if the integral kernel matrix $\{\mathbf{K^{VV_0}}\}$ satisfies the partial differential equations

$$\sum_{\beta=1}^{2} D^V_{\alpha\beta}(r)K^{VV_0}_{\beta\gamma}(r,r')=\sum_{\beta=1}^{2} D^{V_0}_{\gamma\beta}(r')K^{VV_0}_{\alpha\beta}(r,r'), \tag{7}$$

with the boundary conditions

$$K^{VV_0}_{\alpha\beta}(r=0,r')=K^{VV_0}_{\alpha\beta}(r,r'=0)=0. \tag{8}$$

The potential matrix then is determined [10] by the integral kernel matrix

$$V_{\alpha\beta}(r)=V^0_{\alpha\beta}(r)-\frac{2}{r}\frac{\hbar^2}{2\mu_\alpha}\frac{d}{dr}\left[\frac{K^{VV_0}_{\alpha\beta}(r,r)}{r}\right]. \tag{9}$$

An integral kernel matrix that solves Eq. (7) with the constraint of Eq. (8) can be expanded in the radial wave functions $R^I_{\alpha n}(r)$ and $R^{0I}_{\alpha n}(r)$, with spectral coefficients $c^I_{nn'}$, as

$$K^{VV_0}_{\alpha\beta}(r,r')=\sum_{I=0}^{\infty}\sum_{n,n'=1}^{2} c^I_{nn'}R^I_{\alpha n}(r)R^{0I}_{\beta n'}(r'), \tag{10}$$

where the sum over the total angular momentum I might include nonphysical (noninteger) values. Introducing this kernel matrix into Eq. (6) leads to the fundamental equations for the solution of the inverse scattering problem,

$$R^I_{\alpha n}(r)=R^{0I}_{\alpha n}(r)-\sum_{I'=0}^{\infty}\sum_{n'',n'=1}^{2} R^{I'}_{\alpha n''}(r)c^{I'}_{n''n'}L^{I'I}_{n'n}(r), \tag{11}$$

where the matrix $\{\mathbf{L}^{II'}\}$ is completely determined by the known reference solutions,

$$L^{I'I}_{n'n}(r)=\sum_{\beta=1}^{2}\int_0^r R^{0I'}_{\beta n'}(r')R^{0I}_{\beta n}(r')\frac{1}{r'^2}dr'. \tag{12}$$

The ISP then is solved by repeated use of Eq. (11). In a first step, the known asymptotic behavior of the wave functions $R^I_{\alpha n}(r>R_{int})$, as determined by the S matrix, is used to calculate the unknown spectral coefficients $c^{I'}_{n''n'}$. Once these are known, Eq. (11) is used again to calculate the wave functions $R^I_{\alpha n}(r_i)$ at discrete radii r_i in the region of nuclear interaction $0<r_i<R_{int}$. With those known wave functions

and spectral coefficients, the integral kernel matrix can be calculated from Eq. (10) and the potential matrix thereafter by use of Eq. (9).

IV. TRANSFORMATION OF THE *S* MATRIX TO AN ASYMPTOTIC CONSTANT POTENTIAL

For analysis of charged particle scattering, the natural choice for the reference potential is the Coulomb potential [11]; the reference solutions of Eq. (4) then being Coulomb functions. Asymptotically the difference between the reference potential and the sought potential [defined by Eq. (9)] then will tend to zero. However this choice involves a reference potential that has a singularity at the origin. It helps then to make a transformation of the *S* matrix which reduces the case of charged particle scattering to one equivalent to neutral particle scattering [8]; a method that can be applied in the case of transfer reactions.

We consider the *S* matrix $\{\mathbf{S}^C\}$, which belongs to the potential matrix

$$V^C_{\alpha\beta}(r)=\begin{cases} V_{\alpha\beta}(r): & r<r_C \\ \dfrac{Z^\alpha_p Z^\alpha_t e^2}{r}\delta_{\alpha\beta}: & r\geqslant r_C, \end{cases} \tag{13}$$

where the radius $r_C \geqslant R_{int}$ lies outside the region of nuclear interactions. The asymptotic solutions from solving Eq. (2) with this potential, can be written in terms of incoming and outgoing Coulomb waves,

$$T^I_{\alpha n}(k_\alpha r)=\frac{i}{2}e^{i\sigma^I_\alpha}\sqrt{\frac{k_n}{k_\alpha}}[H^*_I(k_\alpha r)\,\delta_{\alpha n}-S^{IC}_{\alpha n}H_I(k_\alpha r)], \quad r>R_{int}, \tag{14}$$

where $H_I(r)=G_I(r)+iF_I(r)$ with G_I and F_I being the Coulomb functions that are irregular and regular at the origin respectively, σ^I_α are the channel Coulomb phases, and

$$k_\alpha=\sqrt{\frac{2\mu_\alpha}{\hbar^2}(E-\varepsilon_\alpha)}, \tag{15}$$

are the channel wave numbers. The asterisk (*) in Eq. (14) denotes complex conjugation.

For large angular momenta *I*, the *S* matrix tends to the unit matrix,

$$S^I_{\alpha n}\to\delta_{\alpha n} \quad (I\to\infty), \tag{16}$$

for which the wave function defined by Eq. (14) then tends to the regular Coulomb function at a rate determined by the wave number k_α. The larger k_α the more partial waves contribute significantly (for the chosen numerical precision) to the scattering. Note that as k_α depends on the reduced mass as well as on the channel energy, the wave numbers in each channel can be quite different.

The idea of the transformation is to replace the potential matrix $\{\mathbf{V}^C(r)\}$ for radii larger than r_C by the constant potential matrix $\{\mathbf{V}^C(r_C)\}$. The value of this constant matrix corresponds to the values of Eq. (13) at the radius r_C,

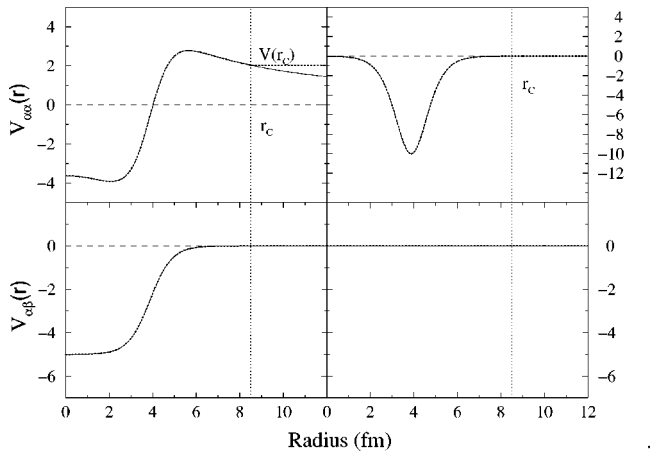

FIG. 1. Schematic representation of the potential matrix $\{\mathbf{V}^C(r)\}$ (full curve) and $\{\mathbf{V}^B(r)\}$ (dotted curve). The two vertical lines show the cutoff radius, r_C. The real and imaginary part are shown in the left and right columns, respectively. The upper half of the figure depicts the diagonal element $V_{\alpha\alpha}$, while the lower half shows the transfer coupling potential $V_{\alpha\beta}$.

$$V^B_{\alpha\beta}(r)=\begin{cases} V^C_{\alpha\beta}(r)=V_{\alpha\beta}(r) & r<r_C \\ V^C_{\alpha\beta}(r_C)=[Z^\alpha_p Z^\alpha_t e^2]/r_C\delta_{\alpha\beta} & r\geqslant r_C. \end{cases} \tag{17}$$

Schematically we show by the solid curves in Fig. 1, the expected forms of the potential matrix $V^C_{\alpha\beta}(r)$ and the change to the input potentials is depicted therein by the dotted curves. As the charge numbers are channel dependent, $\{\mathbf{V}^C(r_C)\}$ has different values in each channel. The asymptotic wave function obtained on solving Eq. (2) with the potential given in Eq. (17), is written in the form of incoming and outgoing spherical Hankel functions as

$$R^I_{\alpha n}(k^B_\alpha r)=\frac{1}{2}ir\sqrt{k^B_n k^B_\alpha}[h^-_I(k^B_\alpha r)\,\delta_{\alpha n}-S^{IB}_{\alpha n}h^+_I(k^B_\alpha r)], \tag{18}$$

where k^B_α are new channel wave numbers,

$$k^B_\alpha=\sqrt{\frac{2\mu_\alpha}{\hbar^2}(E^B_\alpha-\varepsilon_\alpha)}, \quad E^B_\alpha=E-\frac{Z^\alpha_p Z^\alpha_t e^2}{r_C}. \tag{19}$$

From the given *S* matrix $\{\mathbf{S}^C\}$, the new *S* matrix $\{\mathbf{S}^B\}$ can be calculated by fitting the wave function given by Eqs. (14) and its derivative, to the wave function of Eq. (18) and its derivative, i.e.,

$$\sum_{n'=1}^{2} e^{i\sigma^I_\alpha}\sqrt{\frac{k_{n'}}{k_\alpha}}[H^*_I(k_\alpha r_C)\,\delta_{\alpha n'}-S^{IC}_{\alpha n'}H_I(k_\alpha r_C)]D^I_{n'n} = \sqrt{k^B_n k^B_\alpha}r_C[h^-_I(k^B_\alpha r_C)\,\delta_{\alpha n}-S^{IB}_{\alpha n}h^+_I(k^B_\alpha r_C)] \tag{20}$$

and

$$\sum_{n'=1}^{2} e^{i\sigma_\alpha^I}\sqrt{\frac{k_{n'}}{k_\alpha}}\frac{d}{dr}\bigg|_{r=r_C}[H_I^*(k_\alpha r)\delta_{\alpha n'}-S^{IC}_{\alpha n'}H_I(k_\alpha r)]D^I_{n'n}$$

$$=\sqrt{k_n^B k_\alpha^B}\,\frac{d}{dr}\bigg|_{r=r_C}\{r[h_I^-(k_\alpha^B r)\delta_{\alpha n}-S^{IB}_{\alpha n}h_I^+(k_\alpha^B r)]\}. \quad (21)$$

For every total angular momentum I, these form an eight equation set for the determination of the four coefficients, $D^I_{nn'}$, and the four new S matrix elements, $S^{IB}_{\alpha n}$.

The new S matrix $\{\mathbf{S}^{IB}\}$, together with the new wave numbers k^B_α and the new channel dependent center of mass energies E^B_α, now serve as input for the ISP with neutral particles. As the asymptotic constant potential energy was added to the channel energy, the resulting inversion potential then must be shifted by that value.

Note that this transformation scheme is not restricted to just the Coulomb interaction. Rather it is valid for all forms of asymptotic potential matrices with known asymptotic solutions.

V. SOLUTION OF THE ISP FOR NEUTRAL PARTICLE SCATTERING

For neutral particle scattering, the optimal choice for the reference potential is $V^0_{\alpha\beta}(r)=0$ [1,2]. The solutions of the reference Schrödinger equations, Eq. (4), then are the spherical Riccati-Bessel functions,

$$R^{0I}_{\alpha n}(r)=T^{0I}_{\alpha n}(r):=k_\alpha r j_I(k_\alpha r)\delta_{\alpha n}, \quad (22)$$

and the asymptotic solutions of Eq. (2) are determined by the given (or transformed) S matrix,

$$T^I_{\alpha n}(r\geqslant R_{int})=\frac{i}{2}r\ \sqrt{k_n k_\alpha}[h_I^-(k_\alpha r)\delta_{\alpha n}-S^I_{\alpha n}h_I^+(k_\alpha r)]. \quad (23)$$

The wave functions $R^I_{\alpha n}(r)$ in channel α can then be specified as a superposition of these degenerate solutions, i.e.,

$$R^I_{\alpha n}(r)=\sum_{n'=1}^{2} A^I_{nn'}T^I_{\alpha n'}(r). \quad (24)$$

Introducing the wave functions of Eqs. (22) and (24) into Eq. (11) gives the coupled set of equations,

$$\sum_{n'=1}^{2}\left(T^I_{\alpha n'}(r)A^I_{n'n}+\sum_{I'=0}^{I_{\max}}T^{I'}_{\alpha n'}(r)b^{I'}_{n'n}L_n^{I'I}(r)\right)=T^{0I}_{\alpha n}(r), \quad (25)$$

with the new matrices

$$L_n^{II'}(r)=k_n^2\int_0^r j_I(k_n r')j_{I'}(k_n r')dr' \quad (26)$$

and

$$b^I_{nn'}=\sum_{n''=1}^{2} A^I_{nn''}\ c^I_{n''n'}. \quad (27)$$

To get a finite set of equations, the sum over the angular momentum I is limited to $I_{\max}$. The effect of this limitation has been discussed in detail in earlier works [9,12]. Then Eq. (25) is used twice. First, Eq. (25) is solved outside of the interaction region at two Newton radii, $r_1, r_2 > R_{int}$. Assuming the angular momentum step size is ΔI, this gives $8\times(I_{\max}+1)/\Delta I$ equations from which calculation of the unknown coefficient matrices $\{\mathbf{A}\}$ and $\{\mathbf{b}\}$ is feasible. Once these matrices are known, Eq. (25) is solved at discrete equidistant radii $0<r_i<R_{int}$. For each radius r_i and each channel α there are $2\times(I_{\max}+1)/\Delta I$ equations for the calculation of the solutions $T^I_{\alpha n}(r_i)$.

Then the integral kernel matrix can be obtained from Eq. (10) as

$$K^{VV_0}_{\alpha\beta}(r,r')=\sum_{I=0}^{I_{\max}}\sum_{n=1}^{2} b^I_{n\beta}T^I_{\alpha n}(r)k_\beta r j_I(k_\beta r), \quad (28)$$

with which, subsequently, the potential matrix is obtained by using Eq. (9).

Note that Eq. (25) cannot be solved independently for each channel $\alpha=1,2$ in the first step as the set of equations then splits in two uncoupled subsets, one of which forms an homogeneous matrix equation with a nonzero determinant. Consequently, the complete S matrix must be known.

VI. APPLICATION TO AN ANALYTIC MODEL POTENTIAL

As a first test of the new inversion method, we consider the coupled scattering system

$$\begin{pmatrix} {}^{16}\mathrm{O}(\alpha,\alpha){}^{16}\mathrm{O} & {}^{16}\mathrm{O}(\alpha,{}^{8}\mathrm{Be}){}^{12}\mathrm{C} \\ {}^{12}\mathrm{C}({}^{8}\mathrm{Be},\alpha){}^{16}\mathrm{O} & {}^{12}\mathrm{C}({}^{8}\mathrm{Be},{}^{8}\mathrm{Be}){}^{12}\mathrm{C}\end{pmatrix},$$

in which the two elastic channels $^{16}\mathrm{O}(\alpha,\alpha)^{16}\mathrm{O}$ and $^{12}\mathrm{C}(^{8}\mathrm{Be},^{8}\mathrm{Be})^{12}\mathrm{C}$ are coupled by the α-transfer reactions $^{16}\mathrm{O}(\alpha,^{8}\mathrm{Be})^{12}\mathrm{C}$ and $^{12}\mathrm{C}(^{8}\mathrm{Be},\alpha)^{16}\mathrm{O}$. We require all fragments to be in their ground states and all to have zero spin.

For this test case the input S matrix was generated from analytic potentials (of Woods-Saxon form) for these reactions. For the $^{16}\mathrm{O}(\alpha,\alpha)^{16}\mathrm{O}$ scattering, fitted potential parameters found by Wozniak *et al.* [13] were used. The second elastic channel $^{12}\mathrm{C}(^{8}\mathrm{Be},^{8}\mathrm{Be})^{12}\mathrm{C}$ is not available experimentally as $^{8}\mathrm{Be}$ is not stable in its ground state, decaying into two α particles. Instead, the fitted potential parameters for the reaction $^{12}\mathrm{C}(^{9}\mathrm{Be},^{9}\mathrm{Be})^{12}\mathrm{C}$ given by Wozniak *et al.* [13] were used as an approximation. For the endothermic transfer reaction $^{16}\mathrm{O}(\alpha,^{8}\mathrm{Be})^{12}\mathrm{C}$ (with the Q value of -7.162 MeV [14]), no fitted local optical potentials are available. However, in Ref. [13] angular differential cross sections for different excitation states are shown. The cross section for the transfer reaction of interest, with all fragments in the ground state, is only measured at 18 angles in the region from 17° to 75°. A phase shift analysis of that data at most could yield a

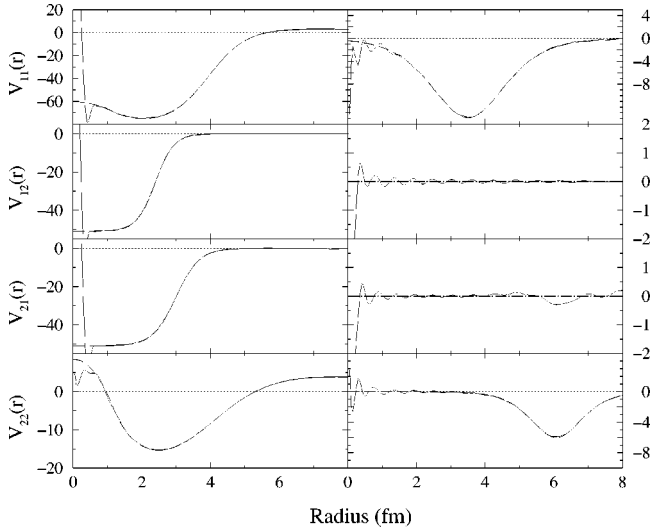

FIG. 2. Comparison of the inverted potential matrix (solid curves) with the analytic input potential matrix (dashed curves) at $E_{\mathrm{c.m.}}=104$ MeV. The real and imaginary parts are shown in the left and right columns, respectively. The potential matrix elements for the reactions $^{16}\mathrm{O}(\alpha,\alpha)^{16}\mathrm{O}$, $^{16}\mathrm{O}(\alpha,^{8}\mathrm{Be})^{12}\mathrm{C}$, $^{12}\mathrm{C}(^{8}\mathrm{Be},\alpha)^{16}\mathrm{O}$, and $^{12}\mathrm{C}(^{8}\mathrm{Be},^{8}\mathrm{Be})^{12}\mathrm{C}$ are shown row-wise from top to bottom.

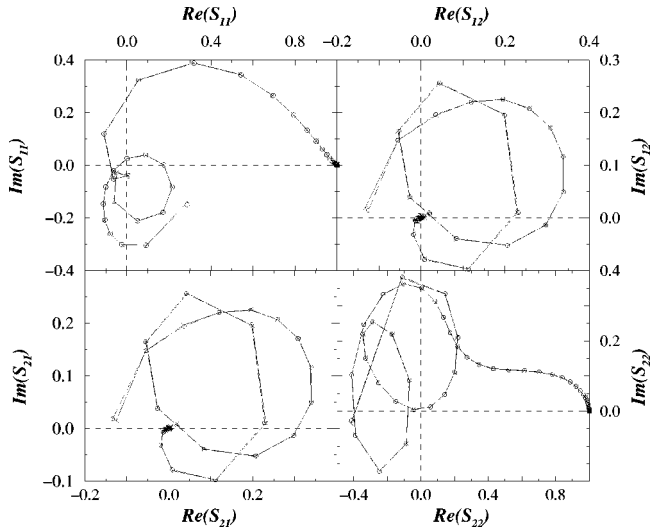

FIG. 3. The Argand diagram of the S matrix found using the inversion potential shown in Fig. 2. The analytic input S matrix is shown by circles connected by the dashed line while the inversion S matrix is portrayed by the crosses connected by the solid line.

maximum of four S matrix elements ($4I_{\max}+3\leqslant N_{\exp}$; see Ref. [15]). Thus a (purely real) Woods-Saxon form was taken for the transfer channel potentials and the potential parameters were obtained by a ''chi-by-eye'' fit of the cross section [10]. Those parameter values were

$$V_z=51\ \mathrm{MeV},\quad R_V=3.0\ \mathrm{fm},\quad a_V^{-1}=3.0\ \mathrm{fm}. \tag{29}$$

For the reverse transfer reaction, $^{12}\mathrm{C}(^{8}\mathrm{Be},\alpha)^{16}\mathrm{O}$, we assume the same interaction potential. The data from which these potential parameters were defined were taken at $E_{\mathrm{c.m.}}=52$ MeV, but for our test study it suits better to consider the scattering system at a higher energy of $E_{\mathrm{c.m.}}=104$ MeV. We have used the potential matrix defined above, however, as it serves the purpose of testing the inversion process and is of a realistic form for such reactions. At 104 MeV sufficient partial waves significantly contribute to the scattering that the resulting inversion potential is quite stable. The input S matrix for the ISP was calculated by numerical integration of the coupled Schrödinger equation, Eq. (2), with a step width of $\Delta r=0.01$ fm. Transformation to an asymptotic constant potential by means of the method that was described in Sec. IV was carried through at a radius r_C of 10.0 fm.

The result of the inversion of this S matrix is shown in Fig. 2. The inversion potentials show the oscillating behavior typically found in many past applications of NS methods, with those oscillations becoming larger close to the origin because of the pole of Eq. (9) at $r=0$ [9]. The inversion calculations were made using Newton radii of 10.1 and 10.2 fm to calculate of the spectral coefficients. With $I_{\max}=50$, 408 coupled equations had to be solved. The wave function and the potential matrix were calculated with a step width of $\Delta r=0.05$ fm in the interval [0.05, 10.2 fm]. At each of these 204 radii, 2×102 coupled equations were solved. As the influence of the choice of the technical inversion parameters has been discussed in detail in earlier works [9,12] we do not cover that aspect again here.

To rate the quality of the inversion potential, a χ^2 test has been performed with

$$(\chi^V_{\alpha\beta})^2=\frac{1}{N}\sum_{i=1}^{N}\left|\frac{V^{inv}_{\alpha\beta}(r_i)-V^{inp}_{\alpha\beta}(r_i)}{1\,\mathrm{MeV}}\right|^2,\quad 1\ \mathrm{fm}\ \leqslant r_i\leqslant R_{int}. \tag{30}$$

The summation has been taken from $r=1$ fm to exclude any significant effect of the pole at $r=0$. The total number of points used in this example was $N=183$. The potential χ^2 values so found using the potentials shown in Fig. 2 are

$$(\chi^V_{11})^2=0.03,\quad (\chi^V_{12})^2=0.02,$$

$$(\chi^V_{21})^2=0.04,\quad \text{and}\quad (\chi^V_{22})^2=0.01. \tag{31}$$

As the elastic potentials in the first and second channel differ significantly in magnitude, the S matrix elements in the first channel tend to unity ($\delta_{\alpha n}$) faster in angular momentum than do those in the second channel. In the first channel, 40 partial waves contribute within the chosen numerical accuracy, whereas in the second channel at least 50 partial waves are required to determine the potential.

In Fig. 3, we compare the analytic input S matrix with that recalculated from the inversion potentials. The four channel sets are shown as Argand diagrams with the input values (at integer I) depicted by the circles. The values calculated using the inversion potentials are portrayed by the crosses. The lines, dashed and solid, respectively, are simply to guide the eye. The overall reproduction is very good as may be measured by a χ^2 value for the S matrix,

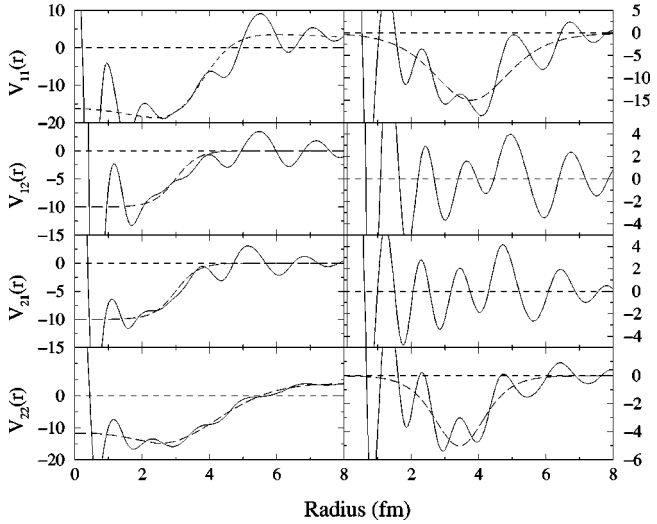

FIG. 4. Comparison of the inverted (solid curves) with the analytic input potential matrix (dashed curves) at $E_{\mathrm{c.m.}}=20$ MeV; with the inversion process involving only integer (physical) partial waves. The notation is as given in Fig. 2.

$$\chi_S^2=\frac{1}{4I_{\max}}\sum_{I=0}^{I_{\max}}\sum_{\alpha,n}^{2}|S_{\alpha n}^{Iinv}-S_{\alpha n}^{Iinp}|^2. \tag{32}$$

For the S matrices shown in Fig. 3, $\chi_S^2=2.0\times10^{-4}$, which corresponds to an average error of less than 1%.

VII. INCLUSION OF NONPHYSICAL S MATRICES

We now consider the situation when relatively few partial waves contribute sensibly in the sums defining observables, as in the case of low energy scattering. In doing so we chose new potential parameters to ensure that the S matrix tends to unity at approximately the same rate in both channels to offset any effects that might be caused by disparate size S matrices in the two channels. For this test, the parameter values chosen are not relevant to the ensuing discussion save that all entries in the potential matrix have similar real strengths, radii, and diffusivities characteristically of 10 MeV, 3 fm, and 0.5 fm, respectively. The two elastic channels have imaginary components still and again they are of derivative Woods-Saxon form. These base potentials are displayed in Fig. 4 by the dashed curves.

We have used this starting potential matrix at the energy of $E_{\mathrm{c.m.}}=20$ MeV to calculate the input S matrix for the given transfer reaction. Within the numerical accuracy, just 20 partial waves now contribute sensibly to the scattering in both channels. The optimum results of the inversion of the associated S matrices specified at integer angular momenta $I=0,1,\ldots,19$ and obtained by minimizing χ_S^2 under variation of the Newton radii, are shown by the solid curves in Fig. 4. The reproduction of the input potential is poor as evidenced by the χ^2 values for the different potential matrix elements which are

$$(\chi_{11}^V)^2=6.6,\quad (\chi_{12}^V)^2=3.3,$$
$$(\chi_{21}^V)^2=1.5,\quad \text{and}\quad (\chi_{22}^V)^2=0.88, \tag{33}$$

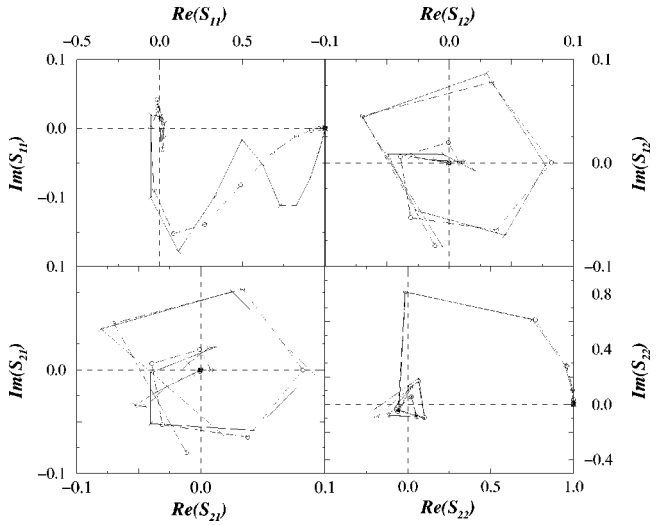

FIG. 5. Argand diagrams of the S matrix found using the inversion potential shown in Fig. 4. The notation is as used in Fig. 3.

when compared with the values typically of order 10^{-2} found for the 104 MeV study. In this case, to calculate the spectral coefficients 160 coupled equations have to be solved. For the wave function, 40 coupled equations are solved at each radius and for each channel. Concomitantly, reproduction of the S matrix elements found by using these inversion potentials is not very good, with the accumulated S-matrix χ^2 value for all channels as specified in Eq. (32) being $\chi_S^2=4.27\times10^{-3}$. The results are shown in Fig. 5 with the notation as used in Fig. 3.

Next we use the analytic potential to calculate the S matrices at half-integer as well as at integer values of angular momentum, thereby having a larger set of equations for the inversion process. The input data are doubled as is the number of coupled equations that have to be solved. The inversion potential matrix obtained with this extended set is shown in Fig. 6, the notation being as used in Fig. 2. It is

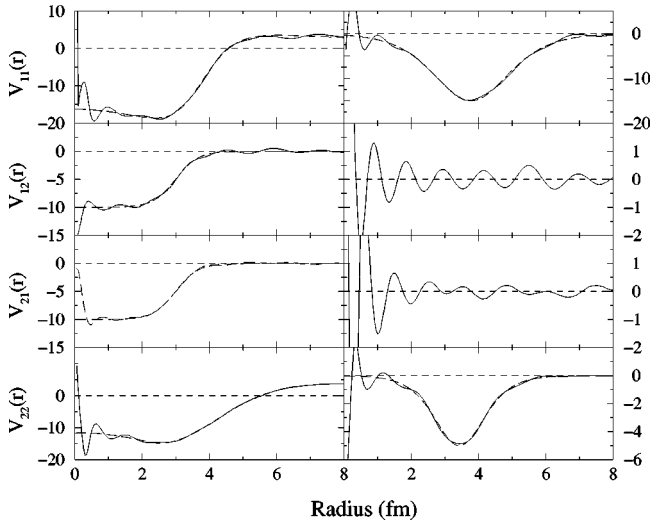

FIG. 6. Same as Fig. 4 but with the inversion process now including S matrix values at half-integer angular momenta.

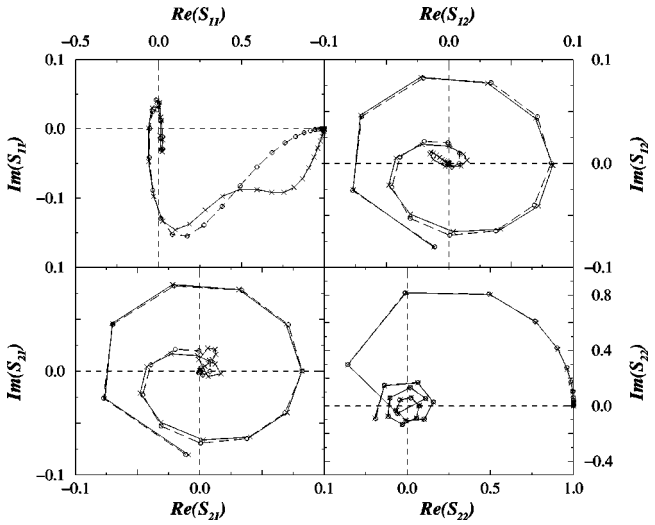

FIG. 7. Argand diagrams of the *S* matrix including values at the half-integer angular momenta and found using the inversion potential shown in Fig. 6. The notation is as used in Fig. 3.

evident that the reproduction of the input potential is significantly improved upon the previous result. The potential χ^2 values are

$$(\chi^V_{11})^2 = 0.06, \quad (\chi^V_{12})^2 = 0.03,$$

$$(\chi^V_{21})^2 = 0.02, \quad \text{and} \quad (\chi^V_{22})^2 = 0.02. \tag{34}$$

Despite this considerable improvement over the first test case run, reproduction of the *S* matrix elements still does not match the quality achieved with the 104 MeV example. The results of the 20 MeV calculations are shown in Fig. 7 and the agreement of the inversion result is rated by an *S*-matrix χ^2_S value of 7.94×10^{-4}. Thus we included the *S* matrix values at quarter integer partial waves as well, again doubling the input data set and the number of coupled equations to be solved. In fact, 672 coupled equations were used to define the coefficient matrices and 168 for the wave functions. The resulting inversion potential matrix is an improvement upon the previous ones as is evident from the comparison given in Fig. 8 and for which

$$(\chi^V_{11})^2 = 0.02, \quad (\chi^V_{12})^2 = 0.05,$$

$$(\chi^V_{21})^2 = 0.01, \quad \text{and} \quad (\chi^V_{22})^2 = 0.02. \tag{35}$$

The *S* matrix elements are now reproduced with an accuracy comparable to that found before with the 104 MeV example and which is shown in Fig. 9.

The results we have shown in this paper were all sensitive to the choice of the technical parameters, $I_{\max}$ and the Newton radii r_1, r_2. The latter had to be specified to an accuracy of 10^{-2} fm to give an optimum χ^2_S. All coupled equations of the ISP were solved by means of a singular value decomposition method, in which the tolerance was taken as 10^{-16}.

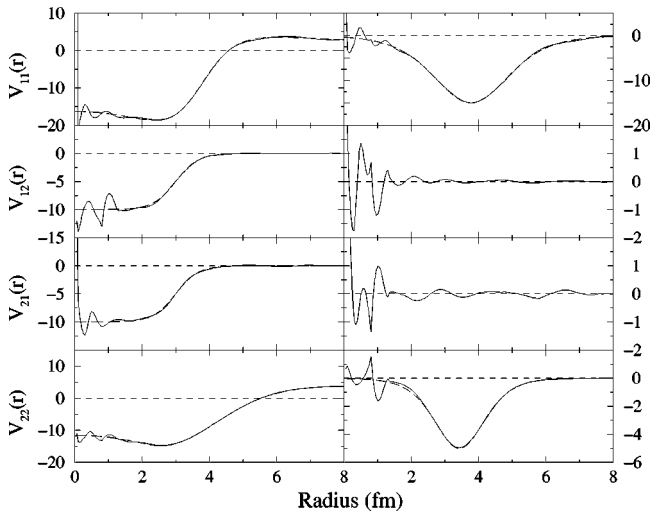

FIG. 8. Same as Fig. 6 but with the inversion now including *S* matrix values at quarter integer values of angular momenta.

VIII. SUMMARY AND CONCLUSIONS

We have specified an exact inversion method for the solution of the inverse scattering problem for transfer reactions. In a first application we used an *S* matrix ascertained from optical model potentials that are characteristic of scattering from the system of interest, and at an energy for which a sufficiently large number of partial waves contribute. The reproduction of the input potentials, and of the input *S* matrix elements found using the inversion potentials, are very good. In a second application we studied the attributes of the inversion potential in the case that only few partial waves contribute to the scattering. Restricting the inversion calculation to use only the physical (integer partial wave) *S* matrix elements gave quite poor results. Including *S* matrices defined at nonphysical (noninteger) angular momenta however, led to quite good reproductions.

Thus, for the first time, direct application of a coupled

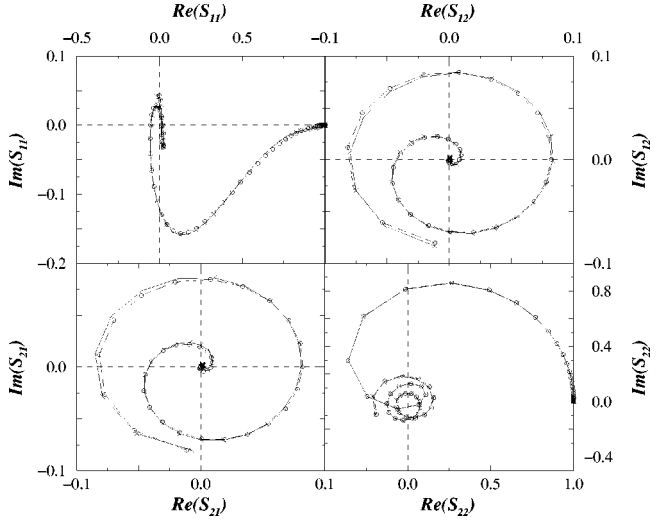

FIG. 9. Argand diagrams of the *S* matrix now including values at quarter integer angular momenta, found using the inversion potential shown in Fig. 8. The notation is as used in Fig. 3.

channel ISP at fixed energy to experimental scattering data seems possible. But the step to define the input from actual scattering data still involves major practical difficulties and limitations. The current method has been designed for transfer reactions in which the interactions do not depend on the angular momentum, and all fragments are spinless. Nevertheless there are real examples that fulfill these conditions, as for instance the α transfer reaction discussed in this paper. Next, one needs at least three angular differential cross sections at appropriate energies. Note that the energy in the second channel is $E_{\text{c.m.}}-Q$ where Q is the Q value of transfer reaction. That data should be accurate and measured at sufficiently many angles and for two elastic, and one transfer channel as the fourth element of the input S matrix can be obtained by symmetry ($S_{21}=S_{12}$). To assure that only the case where all fragments remain in the ground state is important, the scattering energy may need to be kept reasonably low. But then only few partial waves may contribute significantly, and inclusion of S matrix elements at nonphysical angular momenta may be required. Considering the form of the S matrices plotted in our figures, the question remains open as to how these values are to be obtained from the S matrices specified at physical angular momentum values. It has been demonstrated [9] that the interpolation of the S matrix with a rational form is not necessarily reliable. In fact, albeit the rational form might be a physically motivated interpolation, it did not give the correct progression of the S matrix to be connected with the actual underlying interaction.

ACKNOWLEDGMENTS

M.E. and K.A. gratefully acknowledge the support of the Australian Research Council. This work has also been supported partially by the D.F.G. (Bonn) in a collaboration project between the Universities of Gießen and Budapest. B.A. also acknowledges the partial support of O.T.K.A., and M.E. is grateful to Professor W. Scheid of the Justus-Liebig-Universität, Gießen for many valuable discussions.

[1] M. Eberspächer, B. Apagya, and W. Scheid, Phys. Rev. Lett. **77**, 1921 (1996).
[2] M. Münchow and W. Scheid, Phys. Rev. Lett. **44**, 1299 (1980).
[3] *Quantum Inversion Theory and Applications*, Lecture Notes in Physics Vol. 427, edited by H. V. von Geramb (Springer-Verlag, Berlin, 1993).
[4] *Inverse and Algebraic Quantum Scattering Theory*, Lecture Notes in Physics Vol. 488, edited by B. Apagyi, G. Endrédi, and P. Lévay (Springer-Verlag, Berlin, 1997).
[5] R. G. Newton, J. Math. Phys. **3**, 75 (1966); P. C. Sabatier, *ibid.* **7**, 1515 (1966); R. G. Newton, *Scattering of Waves and Particles*, 2nd ed. (Springer-Verlag, New York, 1982); K. Chadan and P. C. Sabatier, *Inverse Problems in Quantum Scattering Theory*, 2nd ed. (Springer-Verlag, New York, 1989).
[6] M. Eberspächer, K. Amos, W. Scheid, and B. Apagyi, J. Phys. G **26**, 1065 (2000).
[7] K. E. May, M. Münchow, and W. Scheid, Phys. Lett. **141B**, 1 (1984).
[8] M. Eberspächer and W. Scheid, J. Math. Phys. **39**, 3061 (1998).
[9] M. Eberspächer, K. Amos, and B. Apagyi, Phys. Rev. C **61**, 064605 (2000).
[10] M. Eberspächer, Ph.D. thesis, Gießen, Germany, 1999.
[11] K.-E. May, Diploma thesis, Gießen, Germany, 1984.
[12] M. Eberspächer, B. Apagyi, and W. Scheid, in *Inverse and Algebraic Quantum Scattering Theory* (Ref. [4]), p. 98.
[13] G. J. Wozniak, D. P. Stahel, J. Cerny, and N. A. Jelly, Phys. Rev. C **14**, 815 (1976).
[14] F. Ajzenberg-Selove, Nucl. Phys. **A460**, 1 (1986).
[15] C. Marty, in *Resonances in Heavy Ion Reactions*, Lecture Notes in Physics Vol. 156, edited by K. A. Eberhard (Springer-Verlag, New York, 1982), p. 216.